Earthquake Engineering, Tenth World Conference © 1992 Balkema, Rotterdam. ISBN 90 5410 060 5

Seismic response of alluvial valleys for incident P, S and Rayleigh waves: A boundary integral formulation

F.J. Sánchez-Sesma
Instituto de Ingeniería, UNAM & Centro de Investigación Sísmica, FJBS, Mexico

J. Ramos-Martínez
Instituto de Ingeniería, UNAM & Instituto de Geofísica, UNAM, Mexico

M. Campillo
Université Joseph Fourier, Grenoble, France

ABSTRACT: A boundary integral formulation is applied to model the seismic response of alluvial valleys under incident P, S and Rayleigh waves. The integral representations used for diffracted and refracted elastic fields are of single-layer type. This approach is called indirect BEM in the literature as the sources strengths should be obtained as an intermediate step. However, it provides far more insight on the physics of the problem than the direct approaches. This is because diffracted waves are constructed at he boundarles from which they are radiated. The two-dimensional response of a very soft parabolic valley is studied. Results are displayed in both frequency and time domains. These results show the significant influence of locally generated surface waves in seismic response and suggest practical approximations.

1. INTRODUCTION

It is now widely accepted the contribution of local topographic and the geological conditions to amplification of ground motion during earthquakes. The subject has received attention during the last two decades and significant progress in the evaluation of such effects has been achieved (see Sánchez-Sesma, 1987 and Aki, 1988 for recent reviews). On the other hand, recent earthquakes have evinced the great significance of site effects (e.g. Vidale y Helmberger, 1988: Campillo et al., 1988).

In a pioneering work, Aki and Larner (1970) introduced a numerical method based on a discrete superposition of homogeneous and inhomogeneous plane waves. Using this technique, Bard and Bouchon (1980a,b; 1985) studied alluvial valleys and pointed out the significant role of sediment-induced surface waves in the valleys' response and the resonant characteristics of these configurations as well. The Aki-Larner technique is the departure of discrete wavenumber approximations.

The combination of discrete wavenumber expansions for Green's functions (Bouchon and Aki, 1977) with boundary integral representations has been successful in various studies of site effects. In some of them source distributions at the boundaries are used (e.g. Bouchon *et al.*, 1989) whereas others make use of Somigliana representation theorem (e.g. Kawase and Aki, 1989; Papageorgiou and Kim, 1991). These are discrete wavenumber versions of BEM, indirect and direct, respectively. However, this combination requires considerable amount of computer resources. An alternative approach may be welcomed for many applications. Such alternative could be the BEM, either direct or indirect, with analytical Green's functions. In a recent work Zhang and Chopra (1991) applied a direct BEM to model the ground motion at a three-dimensional topography.

In this work the indirect BEM is applied to study ground motion on alluvial valleys under incident *P*, *S* and Rayleigh waves. In our approach diffracted waves are constructed at the boundaries from which they are radiated. Therefore, it can be regarded as a numerical realization of Huygens' principle. This is in fact an improvement over a boundary method that has been used to deal with various problems of diffraction of elastic waves (e.g. Sánchez-Sesma and Esquivel, 1979; Luco *et al.* 1990). In its many variants, such technique is based upon the superposition of solutions for *sources* with their singularities placed *outside* the region of interest. However, in the applications, the location of sources requires particular care and the trial and error process needed is difficult to apply, particularly when many frequencies are to be computed.

As the singularities of Green's functions are integrable (see e.g. Kobayashi, 1987; Manolis and Beskos 1988) we put the sources at the boundary and properly consider their effects. In this way, the uncertainty about the location of sources is eliminated. Therefore, our indirect BEM approach retains the physical insight of source method, with the benefits of analytical integration of *exact* Green's functions.

In what follows, the single layer boundary representation of elastic wave fields is briefly described and illustrated with the res-

ponse of a shallow parabolic soft alluvial deposit in a half-space. Transfer functions are given in a frequency-space description which suggests approximations of practical interest. Results are combined to produce a quasi three-dimensional time response in which locally generated Love and Rayleigh surface waves produce rotating polarization patterns.

2. AN INTEGRAL REPRESENTATION

Consider the domain V and its boundary S. If an elastic material occupies such a region, the harmonic displacement field can be written, neglecting body forces, by means of the single layer boundary integral

$$u_i(\mathbf{x}) = \int_S \phi_j(\xi) G_{ij}(\mathbf{x},\xi) dS_\xi \qquad (1)$$

where $u_i(\mathbf{x})$=ith component of displacement at $\mathbf{x}$, $G_{ij}(\mathbf{x},\xi)$=Green function, i.e. the displacement in the direction i at point $\mathbf{x}$ due to the application of a unit force in the direction j at point ξ, $\phi_j(\xi)$=force density in direction j.

This integral representation allows computation of stresses and tractions by application of Hooke's law except at boundary singularities, i.e. when $\mathbf{x}=\xi$ on the boundary. By a limiting process based on equilibrium considerations it is possible to write, for $\mathbf{x}$ on S that

$$t_i(\mathbf{x}) = c\,\phi_i(\mathbf{x}) + \int_S \phi_j(\xi) T_{ij}(\mathbf{x},\xi) dS_\xi \qquad (2)$$

where t_i= ith component of traction at the boundary, c= 0.5 if $\mathbf{x}$ tends to S from inside and c= -0.5 if $\mathbf{x}$ tends to S from outside, $T_{ij}(\mathbf{x},\xi)$= traction Green function, i.e. the traction in the direction i at point $\mathbf{x}$ on the boundary with normal $\mathbf{n}(\mathbf{x})$ (assumed to be specified and pointing outside if $\mathbf{x}$ is at S) due to the application of a unit force in the direction j applied at ξ. The first term of the right hand side must be dropped if $\mathbf{x}$ is not at S. This result has also been found by Kupradze (1963). In its scalar version, the result appeared first in a paper by Fredholm in 1900 (Webster, 1955).

Equations 1 and 2 are the basis of our approach. Although indirect it allows direct interpretation of the physical quantities involved. Expressions for Green's functions can be found in the literature (e.g. Kobayashi, 1987 and Sánchez-Sesma and Campillo, 1991). It suffices to say here that the singularity of displacements is either logarithmic or $1/r$ for 2D or 3D problems, respectively. Regarding the tractions, such singularities are explicitly of the form $1/r$ or $1/r^2$.

3. DIFFRACTION BY AN ELASTIC INCLUSION

Consider the elastic half-space, E, with an elastic inclusion, R, as shown in Figure 1 under incidence of elastic waves. The free-surface boundaries of regions E and R are denoted by ∂_{1E} and ∂_{1R}, respectively. The interface $\partial_{2E} = \partial_{2R}$ is the common boundary between them. The ground motion in this irregular configuration comes from the interferences of incoming waves with reflected, diffracted and refracted ones. The total motion in the half-space is the superposition of the *diffracted* waves and the free-field:

$$u_i^E = u_i^{(0)} + u_i^{(d)} \qquad (3)$$

where $u_i^{(0)}$=free-fied displacement, i.e. the solution in the absence of the irregularity.

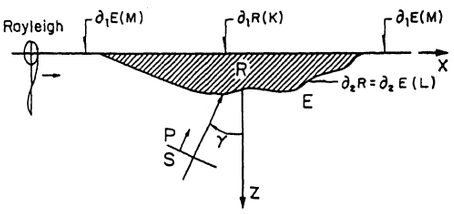

Figure 1. Half-space, E, with an elastic inclusion, R, and incidence of *P*, *S* and Rayleigh waves. The discretization along the interface, the free surface of inclusion and portions of the flat surface of the half-space gives *L*, *K* and *2M* segments.

According to our previous discussion, the diffracted field is given by equation 1 which, with appropriate superscrips to indicate the region of validity, can be written as:

$$u_i^{(d)}(\mathbf{x}) = \int_{\partial E} \phi_j^E(\xi) G_{ij}^E(\mathbf{x},\xi) dS_\xi. \qquad (4)$$

Refracted elastic fields on the inclusion R can be written as:

$$u_i^{(r)}(\mathbf{x}) = \int_{\partial R} \phi_j^R(\xi) G_{ij}^R(\mathbf{x},\xi) dS_\xi. \qquad (5)$$

The traction-free boundary conditions imply

$$t_i^{(0)} + t_i^{(d)} = 0 \qquad \text{on } \partial_1 E \qquad (6)$$

and

$$t_i^{(r)} = 0 \qquad \text{on } \partial_1 R \qquad (7)$$

equations 6 and 7 and those of continuity along the interface lead to a system of integral equations for boundary sources, i.e. those producing diffracted and refracted fields.

4. DISCRETIZATION

In order to solve the resulting system of integral equations we have to discretize them. Let us assume the force densities $\phi_J(\xi)$ constant over each of the boundary segments with equal length ΔS along each appropriate boundary. Assume that M, L and K are the number of segments (elements) along the discretized part of the flat surface of one side, of the irregular interface and of the free surface of region R as depicted in Figure 1. The total number of equations is $4M+4L+2K$ which is the same as the number of unknowns.

To clarify ideas, let us write the discretized versions of equations 1 and 2:

$$u_i(x) = \sum_{j=1}^{N} \phi_j(\xi_j) g_{ij}(x,\xi_j) \qquad (8)$$

where

$$g_{ij}(x, \xi_j) = \int_{\xi_j-\Delta S/2}^{\xi_j+\Delta S/2} G_{ij}(x,\xi) dS_\xi . \qquad (9)$$

and

$$t_i(x) = \sum_{j=1}^{N} \phi_j(\xi_j) t_{ij}(x,\xi_j) \qquad (10)$$

where

$$t_{ij}(x,\xi_i) = \int_{\xi_j-\Delta S/2}^{\xi_j+\Delta S/2} [\, c_{ij}\delta(x_i-\xi) + T_{ij}(x,\xi)]dS. \qquad (11)$$

The integrals in equation 9 are computed numerically with Gaussian integration, except in the case when x is in the neighborhood of ξ_i for which we obtained analytical expressions from the ascending series for Bessel functions (see *e.g.* Abramowitz and Stegun, 1972). Whereas those in equation 11 are also computed numerically except when $x_n=\xi_i$. In this case, we have:

$$t_{ij}(x_n,\xi_n) = 0.5\ \delta_{ij}\ , \qquad (12)$$

because the only contribution to the integral in equation 11 for $n=i$ comes from the Dirac's delta term. The contribution from the tractions Green's tensor is null as long as the discretization segment is a straight line, which is the case assumed here. In fact, it can be verified that, such part of the integrand is a singular odd function on the segment. Therefore, its Cauchy's principal value is zero. The value for t_{ij} in equation 18 can be interpreted as half of the applied unit line force and means that the force is distributed symmetrically for any two half-spaces containing the line of application of the load, regardless of its direction.

Once the values of $\phi_j(\xi_i)$ are known, the diffracted field is computed by the appropriate discretization of equations 4 and 5.

5. NUMERICAL RESULTS

The accuracy of this approach has been verified by Sánchez-Sesma and Campillo (1991) for problems of topographical irregularities and by Ramos-Martínez and Sánchez-Sesma (1991) for the response of alluvial valleys. Excellent agreement was found with published results (e.g. Kawase and Aki, 1989).

The results presented here were obtained using a discretization length L for each of the flat parts, where L=length of the interface, and 10 segments per S wavelength. The results are virtually the same even when such parameter is reduced to 6.

Some results follow for incident S waves, both antiplane SH and inplane SV ones, upon a very soft shallow parabolic valley. The maximum depth is 0.05 times the half width ($h=a/20$) as it is shown in figure 2. Material properties are $\rho_R/\rho_E=1/2$ and $\beta_R/\beta_E=1/4$ for mass density and shear wave velocity ratio, respectively. Poisson ratios of 1/3 and 0.49 were selected for the half-space and the valley. The α/β ratios are then 2 and 7.14, respectively.

We can consider the incidence of a plane S wave with a given incidence angle γ and arbitrary polarization θ (see figure 2) by the simple combination of SH ($\theta = 0$) and SV ($\theta = \pi/2$) responses. Each one will be modulated by sin θ and cos θ, respectively. This allows to study how the propagation of Love and Rayleigh surface waves interact and control the polarization of horizontal motion.

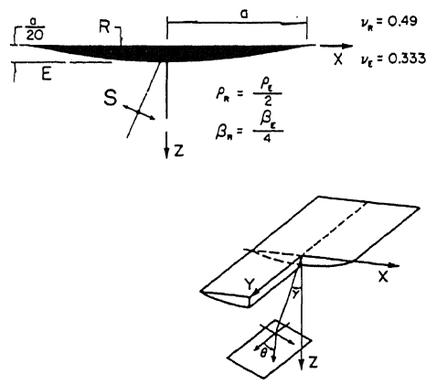

Figure 2. Soft alluvial valley with parabolic interface under incidence of plane S waves. Incidence and polarization angles are represented by γ and θ, respectively. Material properties are $\rho_R/\rho_E=1/2$ and $\beta_R/\beta_E=1/4$ for mass density and shear wave velocity ratios, respectively. Poisson ratios are 1/3 and 0.49 for regions E and R.

Computations were performed in the frequency domain and are shown in figures 3 and 4 for vertical incidence and in figures 5 and 6 for oblique incidence. A great variability of am-

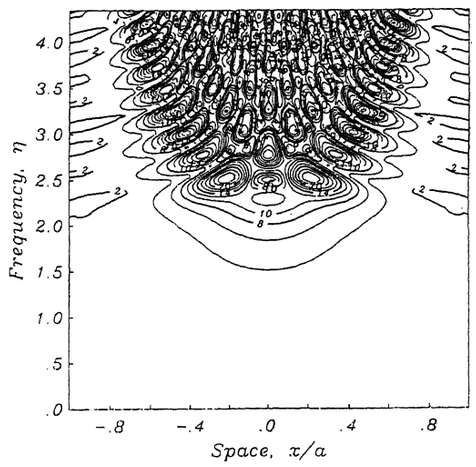

Figure 3. Contour map of transfer function v in the frequency-space domain (f-x) for vertical incidence of *SH waves* upon a shallow parabolic valley. η=normalized frequency.

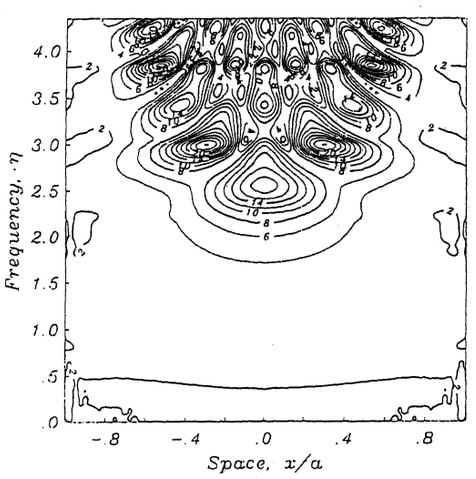

Figure 4. Contour map of transfer function u in the frequency-space domain (f-x) for vertical incidence of *SV waves* upon a shallow parabolic valley. η=normalized frequency.

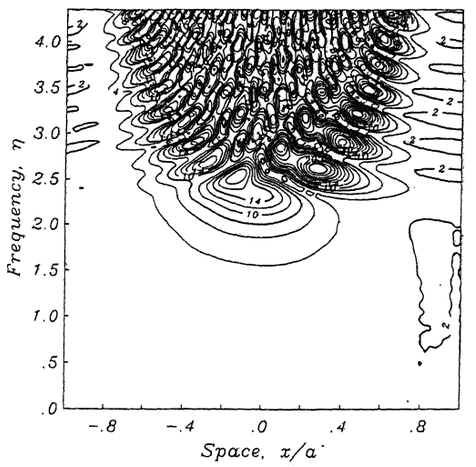

Figure 5. Contour map of transfer function v in the frequency-space domain (f-x) for incidence of 30°of *SH waves* upon a shallow parabolic valley. η=normalized frequency.

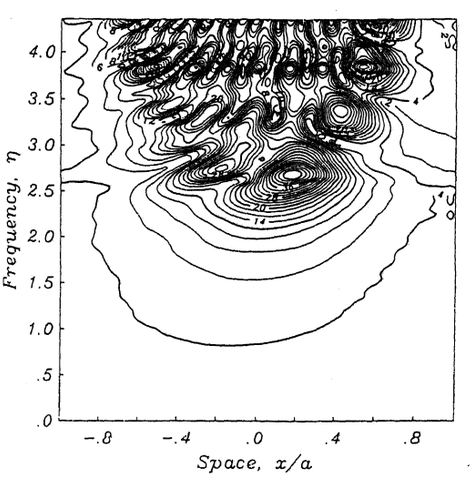

Figure 6. Contour map of transfer function u in the frequency-space domain (f-x) for incidence of 30°incidence of *SV waves* upon a shallow parabolic valley. η=normalized frequency.

plifications in frequency domain can be seen. It is larger for the *SH* case. In both cases horizontal amplification reached more than 25 times the amplitude of incident waves at some receivers. This happens for frequencies larger than about η=2. Note that the one-dimensional shear model predicts a maximum amplification of 16, and for the center of the model that would occur at η=2.5. However, lateral interferences from surface waves strongly modify that. On the other hand, vertical motion for incidence of *SV* waves (not shown here) is significantly excited for frequencies larger than about η=2, giving a value of 10 for η=3.75. In any event, horizontal motion dominates the valley's response for the range of frequencies studied.

These contour maps of transfer functions in the frequency-space domain (f-x) of figures 3 to 6 reveal a fine structure in which lateral propagation plays a significant role for frequencies higher than the one that controls the 1D response at the center. In these results, the maximum amplifications for normalized frequencies larger than η=2.5 occur at the borders of a portion that grows with frequency. Indeed, if we consider that a first resonant frequency

of an associated 1D shear model with the local thickness $h(x)$ is given by $f_0=\beta_R/4h(x)$ which, for this model can be written as

$$\eta_0 = 2.5[1-(x/a)^2]^{-1} ,$$

therefore, the borders of the excited central portion for a given frequency $\eta>2.5$ occur approximately at $x\cong\pm a(1-2.5/\eta)^{1/2}$. Outside this region amplification is moderate. The amplification inside can be very large with a clearly defined resonant behavior. This phenomenon can be explained if we consider that from a given zone of "local" resonance wave propagation is *estimulated* towards deeper parts. Then, amplifications are also controled by surface waves. The maxima show a lateral resonant pattern. Although, in this example we have very small material damping (Q=500) these results suggest that practical approximations can be found to describe the response of shallow, soft alluvial deposits in terms of surface waves.

The results for horizontal displacement amplitude u under vertical incidence of *SV* waves, even with the mode conversions that occur, is similar with fewer maxima than in the *SH* case. This can be explained considering the different behavior of dispersion curves of Love and Rayleigh waves in this model (figure 7).

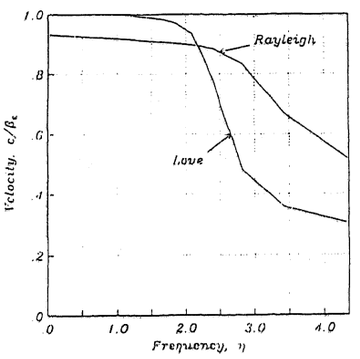

Figure 7. Dispersion curves of surface waves for a one-dimensional model with a depth of 0.05 times the half width of parabolic deposit and the same physical properties.

We computed synthetic seismograms from frequency domain results by using the FFT algorithm. The time variation of incoming wavefield is given by a Ricker wavelet with characteristic period $t_p=0.5t_o$, where $t_o= 2a/\beta_\varepsilon$. For an incidence angle γ =0, Figures 8 and 9 show the synthetics for *SH* and *SV* waves, respectively. These results can be combined to produce a quasi three-dimensional response with the horizontal motion given by the inplane u and antiplane v components, respectively. Figure 10 shows the particle motion and polarigrams for sites across the valley when the polarization angle is θ=45°. The soft layer response produces rotating horizontal polarization patterns.

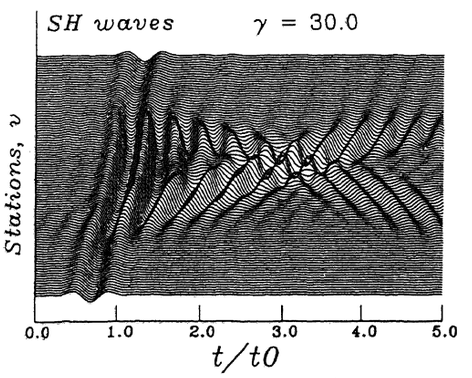

Figure 8. Synthetic seismograms $v(t)$ for incidence of 30° of *SH* waves in 51 stations (from -1.25a to 1.25a) across the surface of the two-dimensional shallow parabolic valley. The incident time signal is a Ricker wavelet with central frequency $\omega_p = 2\pi\beta_\varepsilon/a$.

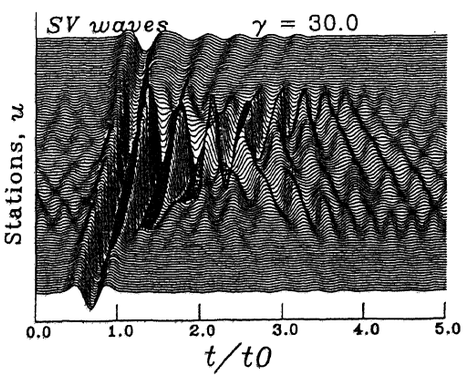

Figure 9. Synthetic seismograms $u(t)$ for incidence of 30°of *SV* waves in 51 stations (from -1.25a to 1.25a) across the surface of the two-dimensional shallow parabolic valley. The incident time signal is a Ricker wavelet with central frequency $\omega_p = 2\pi\beta_\varepsilon/a$.

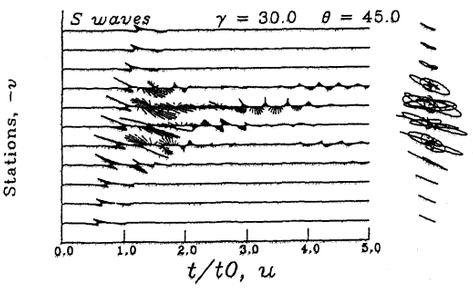

Figure 10. Horizontal polarigrams and particle motion for 11 stations (from -1.25a to 1.25a) across the two-dimensional shallow parabolic valley model. Incidence 30°of *S* waves with polarization angle θ=45°.

6. CONCLUSIONS

An indirect boundary integral formulation for dynamic elasticity has been presented. It is based upon the integral representation of the diffracted elastic waves in terms of single layer boundary sources. Although this approach is called indirect BEM in the literature, it provides far more insight on the physics of diffraction problems than the direct approaches. In addition to the physical insight gained with this method, it appears to be accurate and fast.

A very soft shallow deposit was analized for incident *SH* and *SV* waves. Very large amplifications were found and the contour maps of transfer functions in the frequency-space domain (f-x) reveal a fine structure in which locally generated surface waves play a significant role for frequencies higher than the one that controls the 1D response at the center. The maximum amplifications occur at the borders of a portion that grows with frequency. Such a frequency corresponds to the "local" 1D shear model resonance. As wave propagation is estimulated towards deeper parts, amplifications are also controled by surface waves. These results suggest that practical approximations can be found to describe the response of shallow, soft alluvial deposits in terms of surface waves, Love and Rayleigh for the *SH and SV* cases, respectively.

7. ACKNOWLEDGEMENTS

Thanks are given to M. Bonnet, C. Calderón, S. Chávez-Pérez and L.E. Pérez-Rocha, for their comments and suggestions. This work was partially supported by Departamento del Distrito Federal, Mexico, and by Consejo Nacional de Ciencia y Tecnología, Mexico, under Grant P0523-T9109.

8. REFERENCES

Abramowitz, M. and I.A. Stegun 1972. Handbook of mathematical functions, Dover Publications, New York.

Aki, K. 1988. Local site effects on strong ground motion, in Earthquake Engineering and Soil Dynamics II-Recent advances in ground motion evaluation, J. L. Von Thun (ed.), Geotechnical Special Publication No. 20: 103-155, Am. Soc. Civil Engr., New York.

Aki, K. and K.L. Larner 1970. Surface motion of a layered medium having an irregular interface due to incident plane SH waves. J. Geophys. Res. 75: 1921-1941.

Bard, P.-Y. and M. Bouchon 1980a. The seismic response of sediment-filled valleys. Part 1. The case of incident SH waves. Bull. Seism. Soc. Am. 70: 1263-1286.

Bard, P.-Y. and M. Bouchon 1980b. The seismic response of sediment-filled valleys. Part 2. The case of incident P and SV waves. Bull. Seism. Soc. Am. 70: 1921-1941.

Bard, P.-Y. and M. Bouchon 1985. The two-dimensional resonance of sediment-filled valleys, Bull. Seism. Soc. Am. 75: 519-554.

Bernard, P. and A. Zollo 1989. Inversion of near-source S polarization for parameters of double-couple point sources. Bull. Seism. Soc. Am. 79: 1779-1809.

Bouchon, M. and K. Aki 1977. Discrete wavenumber representation of seismic-source wave fields, Bull. Seism. Soc. Am. 67: 259-277.

Bouchon,M., M. Campillo and S. Gaffet 1989. A boundary integral equation-discrete wavenumber representation method to study wave propagation in multilayered media having irregular interfaces. Geophysics 54: 1134-1140.

Kawase, H. and K. Aki 1989. A study on the response of a soft basin for incident S, P and Rayleigh waves with special reference to the long duration observed in Mexico City. Bull. Seism. Soc. Am. 79: 1361-1382.

Kobayashi, S. 1987. Elastodynamics, in Boundary element methods in mechanics, D.E. Beskos (ed.) North-Holland, Amsterdam.

Luco, J.E., H.L. Wong and F.C.P. De Barros 1990. Three-dimensional response of a cylindrical canyon in a layered half-space. Earthq. Eng. Struct. Dyn. 19: 799-817.

Manolis, G.D. and D.E. Beskos 1988. Boundary Element Methods in Elastodynamics, Unwin Hyman Ltd, London.

Papageorgiou, A.S. and J. Kim 1991. Study of the propagation and amplification of seismic waves in Caracas Valley with reference to the 29 July 1967 earthquake: SH waves. Bull. Seism. Soc. Am. 81: 2214-2233.

Ramos-Martínez, J. and F.J. Sánchez-Sesma 1991. Respuèsta sísmica de valles aluviales usando ecuaciones integrales. Proc IX Congreso Nacional de Ingeniería Sísmica 1: 289-298, Manzanillo, Colima, Mexico, October.

Sánchez-Sesma, F.J. 1987. Site effects on strong ground motion. Int. J. Soil Dyn. Earthquake Eng. 6: 124-132.

Sánchez-Sesma, F.J. and J.A. Esquivel 1979. Ground motion on alluvial valleys under incident plane SH waves. Bull. Seism. Soc. Am., 69: 1107-1120.

Sánchez-Sesma, F.J. and M. Campillo 1991. Diffraction of P,SV and Rayleigh waves by topographical features: a boundary integral formulation, Bull. Seism. Soc. Am. 81: 2234-2253.

Trifunac, M.D. 1971. Surface motion of a semi-cylindrical alluvial valley for incident plane SH waves. Bull. Seism. Soc. Am. 61: 1755-1770.

Webster, A.G. 1955. Partial differential equations in mathematical physics. Dover Publications Inc., New York.

Vidale, J.E. and D.V. Helmberger 1988. Elastic finite-difference modeling of the 1971 San Fernando, California earthquake. Bull. Seism. Soc. Am. 60: 122-141.

Zhang, L. and A.K. Chopra 1991. Three-dimensional analysis of spatially varying ground motions around a uniform canyon in homogeneous half-space, Earthq. Engrg. & Structl. Dyn 20: 911-926.